Chapter 4
Electron Microscopy and Ultrastructures

4.1 Introduction

Electron microscopy in association with physiological, biochemical, and genetical studies has provided information which helps in understanding the complex host-parasite relationship of this disease. With the use of light electron microscopy, and transmission electron microscopy, fine structures of *H. parasitica* have been observed during the process of host penetration, haustorium development, the host-pathogen interface, conidia and conidiophore formation and development, host response and cytology, and genetics of the pathogen.

4.2 Host Penetration

Penetration and haustorial formation in epidermal cells begin 6 h after inoculation (Plate 4.1b, c) (Chou 1970). Appressoria, which look like swollen discs 7–10 μm, across form at the junction of epidermal cells (Plate 4.1b). At this stage, the appressoria and haustoria appear densely granulated, as the spores empty their contents during the process of germination and infection. The penetrating hyphae lay in between the anticlinal cell walls of the two epidermal cells (Plate 4.1c) along with the formation of one or two haustoria, reaching to the adjacent mesophyll cells. After 45 h, intercellular hyphae ramify through more cells and reach the opposite epidermis. At this stage, the haustoria appear broad and conspicuous, reaching 20 μm in length. The intercellular hyphae are about 7 μm, across. Sometimes a sheath can be observed enveloping a fully grown haustorium (Plate 4.1d). The earliest detectable stage of penetration is the formation of penetration hyphae which are as long as the vertical depth of the entire epidermal cell. The thick wall of the appressorium, continuous with the wall of the penetration hypha (Plates 4.1a and 4.3a), has only a thin peripheral layer of cytoplasm. The cell contents migrate into

G. S. Saharan et al., *Downy Mildew Disease of Crucifers: Biology, Ecology and Disease Management*, https://doi.org/10.1007/978-981-10-7500-1_4

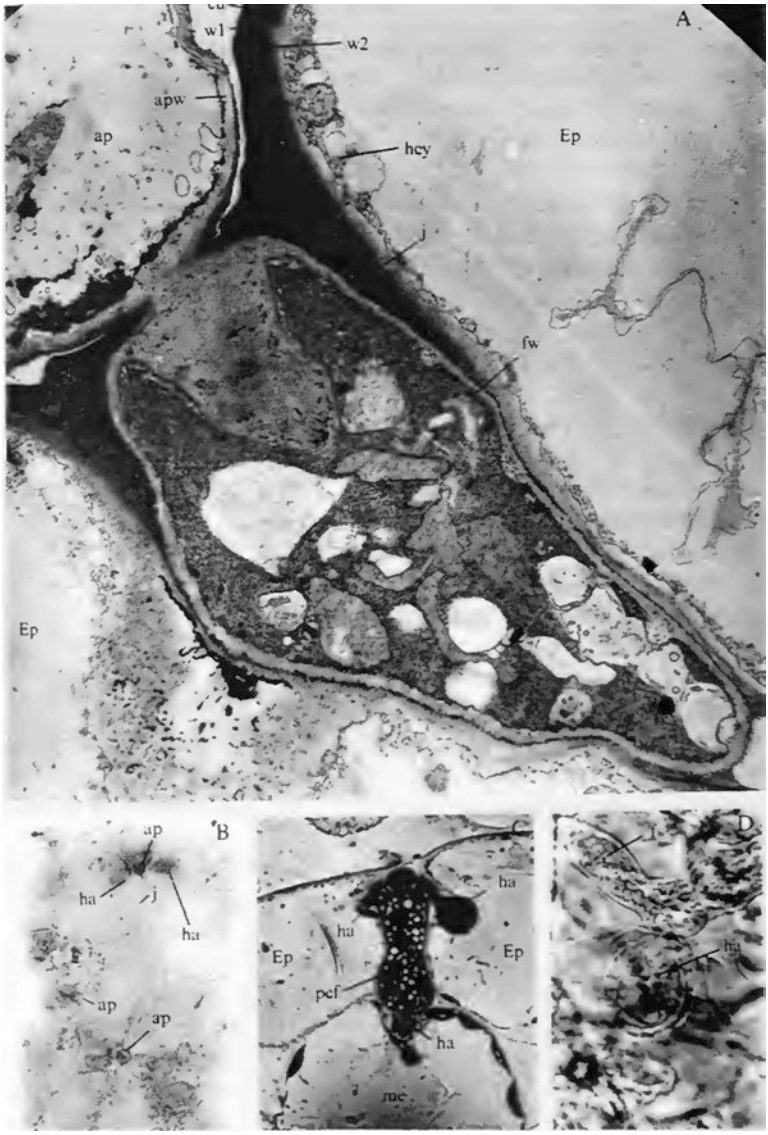

Plate 4.1 (**a**) Electron micrograph of TS of epidermal cells of cabbage cotyledon at 6 h after inoculation showing appressorium (ap) and penetrating hypha of *Hyalo peronospora parasitica* in between the anticlinal walls (j) of host epidermal cells. In one of the cells, a haustorium was formed but the section only shows part of sheath(s). The penetration was cut obliquely, and part of the hyphal wall (arrow pointed) is shown, × 8200; (**b**) photomicrograph of whole mount of a cleared cabbage cotyledon at 6 h after inoculation showing appressorium (ap) formation predominantly at the junction line of epidermal cells × 313; (**c**) photomicrograph CTS of cabbage cotyledon at 6 h after inoculation showing penetration as in A. × 500; (**d**) photomicrograph of whole mount of a cleared cotyledon showing intercellular hypha and haustorium completely ensheathed × 840 (Chou 1970)

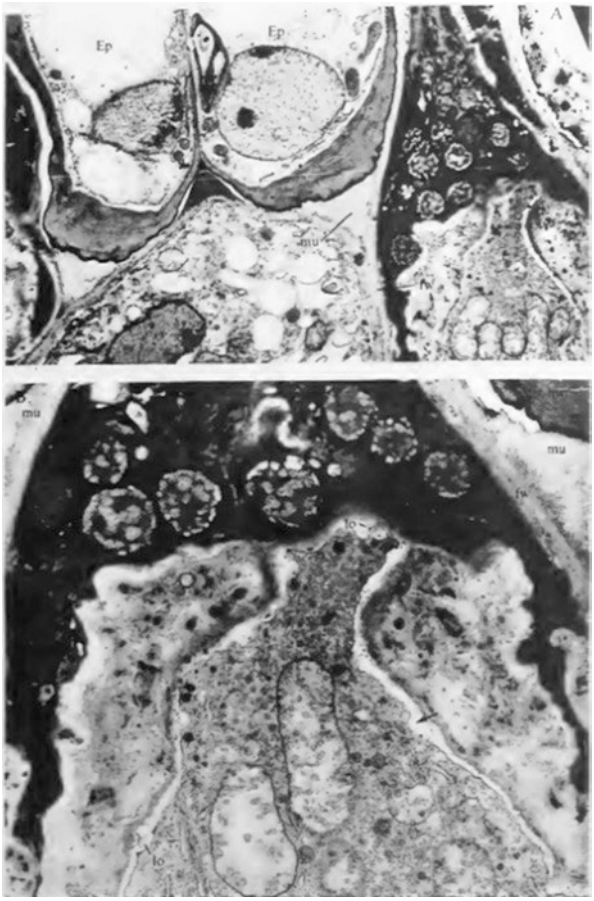

Plate 4.2 (**a**) Electron micrograph of TS of epidermal cells of cabbage cotyledons at 6 h after inoculation showing intercellular hyphae at various stages of penetration to the outside of host epidermis. Arrow points at the spearhead-like thickening of hyphal tip, × 5400; (**b**) electron micrograph of part of outgrowing hypha in between two host epidermal cells showing dieback of hyphal tip and walling-off (arrow pointed) of apparently intact cytoplasm, × 18000 (Chou 1970)

the newly formed penetration hypha. In some cases, the appressorium can be seen to be embedded in an electron-dense, vacuolate material (Plate 4.3b) appearing to be a mucilaginous sheath. This sheath is bound by an outer membrane which adheres to the cuticle of the host epidermis except in the penetration region where it is slightly separated (Plate 4.3b). The penetrating hyphae wedge into the middle lamella between the anticlinal walls of two epidermis cells. The hole in the wall through which the fungus penetrates is 4–5 μm across. After entering the host, the hypha expands to a diameter of 7–8 μm. There is no clearing zone or dissolution of wall material in the immediate vicinity of the penetrating hypha. The penetrating hypha is always seen to be embedded in a moderately electron-dense matrix of the middle lamella (Plates 4.1a and 4.3a). The cuticle breaks and fits closely around the penetrating hypha. No sign of swelling or change in electron density of the cuticle can be detected in the immediate vicinity of the penetration zone (Chou 1970).

After 80 h, hyphal growth develops conidiophores which may be seen coming out from the epidermal cells (Chou 1970). The intercellular hyphae appear to aggre-

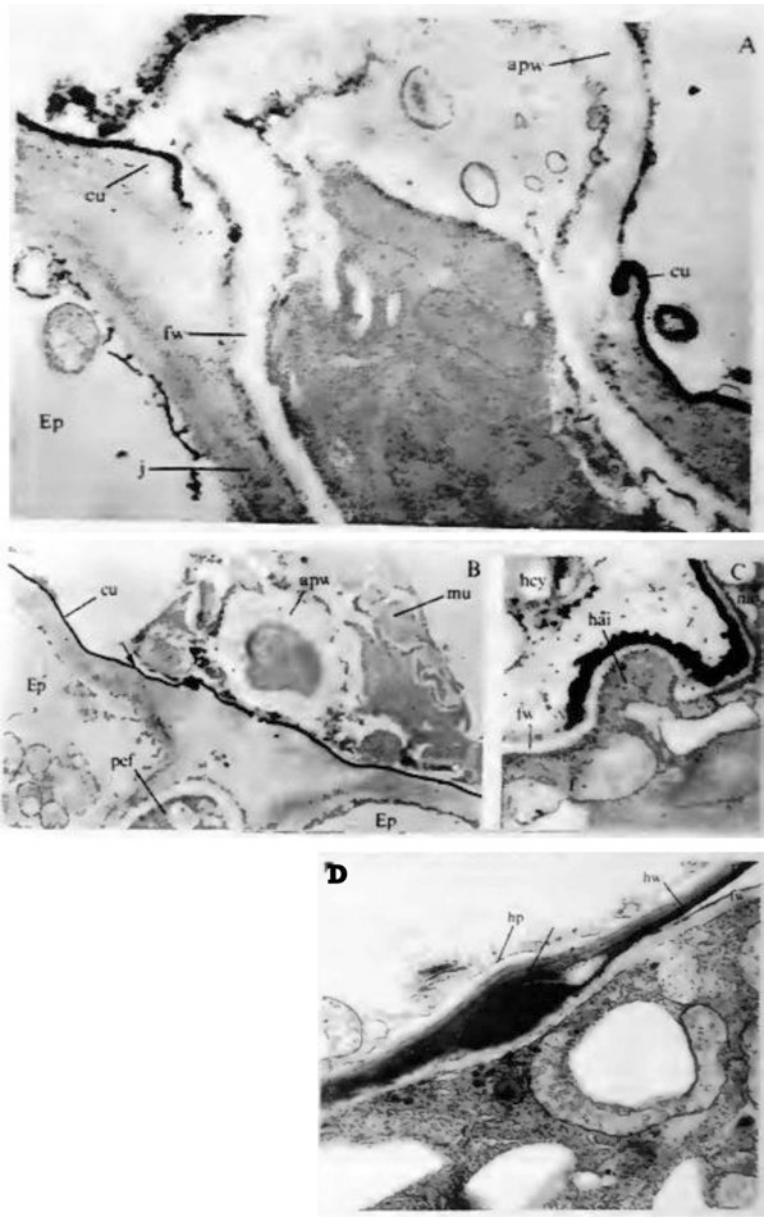

Plate 4.3 (**a**) Electron micrograph of TS of epidermal cells of cabbage cotyledon at 6 h after inoculation. The penetration region was cut medially through showing the appressorium which is almost empty with cytoplasm migrating into the penetrating hypha, × 14400; (**b**) electron micrograph of TS of appressorium and part of host epidermal cells showing the mucilaginous sheath of the appressorium. Membranous boundary of the mucilaginous sheath is shown by arrow, × 6000; (**c**) electron micrograph of section of a haustorium initial in host epidermal cell. Pan of the neck of a fully grown haustorium is shown by its side. Note the hyphal wall is continuous with wall of the intercellular hypha at this stage, × 13800; (**d**) electron micrograph of a section of intercellular hypha and host epidermal cell showing pan of host wall in contact with hypha is swollen and partially eroded (arrow), × 17700 (Chou 1970)

gate beneath the epidermis and grow either through stomata or in between two epidermal cells to the outside of the host tissue (Plate 4.2a). An electron-dense spearhead-like thickening of the hyphal tip is observed to wedge in between two guard cells. This thickening may give rigidity to the hyphal tip for penetration. The hyphae are cemented to each other and also to the host cell walls by an amorphous, moderately electron-dense material, presumably of a mucilaginous nature (Plate 4.2a, b). Hyphae penetrating through the junction of epidermal cells invariably show a dieback of the tip (Plate 4.2a). A new wall is laid down round the remaining living cytoplasm, while a new growing tip is organized to carry on further growth (Plate 4.2b). Large numbers of lomasomes appear around the newly formed walls, and numerous dense vesicles approximately 500–1000 Å in diameter are concentrated in the walled-off cytoplasm.

4.3 Haustorium Development

Host penetration by haustoria of the Peronosporales is usually by boring a narrow canal at the point of contact between the hypha and the host cell wall (Fraymouth 1956). However, according to Chou (1970), it is not possible to find the stage at which the walls of both host and pathogen are perforated prior to haustorial initiation. Localized swelling of the host wall (3X original) is observed in the area of hyphal contact. The swollen area is about 1.5–2 μm long and shows a clearer fibrillar structure, with a partially eroded area (Plate 4.3d). The dimension of the swollen region coincides closely with the size of the hole in the host wall made by the haustorium. These observations strongly suggest that the breach of host wall during haustorium initiation is achieved at least partly by chemical means. A dome-shaped protuberance, about 1 μm in diameter, is formed by the bulging of the wall of intercellular hypha into the lumen of host cell (Plates 4.3c and 4.4a). The host wall is perforated at this stage, and the wall of the haustorium primordium is continuous with that of the intercellular hypha (Plate 4.3c). The haustorium initial is completely enclosed in a mound-like sheath quite distinct from the host wall in structure as well as density. The perforation made by the invading haustorium measures 1–2 μm across. The perforated host wall in most cases remains smooth, but a slight unfolding of the wall to form a short collar-like structure is sometimes observed. The external part of the wall of the haustorial initial consists of a very electron-dense layer varying in thickness from 0.1 to 0.2 μm and exhibiting an undulating surface bounded externally by a thickened membrane (Plates 4.3c and 4.4a) which is presumably the invaginated plasmalemma of the host. The primordial haustoria are filled with homogeneous groundplasm packed with ribosomes. Lomasomes are the only organelles present at this stage. The growth and differentiation of the primordial haustorium is in the form of an elongated neck and expanding head (Plate 4.4b). The sheath seems to burst apart, remaining as a collar-like structure around the neck region (Plate 4.4b).

In a young haustorium, the contents are invariably dense with a high population of ribosomes, a profuse system of endoplasmic reticulum, and relatively few vacuoles (Chou 1970). The dictyosomes occur more frequently, and the mitochondria are strikingly irregular (Plates 4.5, 4.6 and 4.9b). The same pattern of these structures is also present in young penetration hyphae. A complicated membrane system of unknown nature and origin is always present (Plate. 4.10b, c). One type consists of a complicated system of tubules and vesicles enclosed by a unit membrane. The inter-tubular spaces do not contain ribosomes. This organelle looks like a lomasome except that there is no apparent connection with plasmalemma. Another type consists of whorls of closely packed membranes formed in vacuoles (Plate 4.10c). Generally the lomasomes are more or less hemispherical to saucer shaped, about 0.2–0.3 μm in the longer diameter, but occasionally they can extend to 2–3 μm in diameter (Plate 4.6). The tubules and vesicles of lomasomes range from 15 to 80 μm in diameter. The nuclei are about 3–3.5 μm in diameter. As many as three sections of nuclei are observed in one haustorium section (Plate 4.9a). The nuclei envelope consists of a double membrane interrupted by pores. The envelope is very similar in form to the endoplasmic reticulum, and connections between these two are often observed. The endoplasmic reticulum is mainly of the smooth type (Plates 4.9a and 4.6) enlarged in part to form cisternae of various forms. The mitochondria are large (1–2 μm in diameter), usually elongated dumb bell shaped, or irregularly branched (Plates 4.6, 4.9, 4.1a and 4.3d). Those in old haustoria are roundish with a much less dense matrix (Plate 4.9b).

4.4 The Host-Pathogen Interface

The external surface of the haustorial walls always appears to consist of very electron-dense layer (Plates 4.4b, 4.5, 4.6, 4.9a, 4.10a and 4.11c, d) which is well developed at the earliest stage of haustorial development (Chou 1970). The outer region of the hyphal wall can be further differentiated into a well-defined, very dense, and thin outer boundary, about 50–100 Å thick, and an inner less dense zone of rather obscure lateral limit (Plate 4.8e). The hyphal wall thus appears to be a three-layered structure. The zone of apposition of the haustorial wall consists of a well-defined, very dense, and thin outer layer approximately 50–100 Å thick and a broad, slightly less dense inner zone without a well-defined boundary (Plates 4.8d). Chou (1970) proposed that the zone of apposition should be termed as an outer and inner dense zone being both an integral part of the haustorial wall. The surface of the haustorium neck is covered by a dense layer much thicker than that of the rest of the haustorium. Its surface always appears to be deeply roughened with numerous vesicular and tubular extensions (Plates 4.6, 4.7b and 4.11b). Dense granular bodies can sometimes be seen lodged between the surface of the dense layer and the invaginated host plasmalemma and in both of the matrix of the dense layer and of the tubular extension (Plates 4.7a and 4.11b). There is a frequent occurrence of a porous substance of uniform pore diameter (about 200 Å) covering the entire haustorium

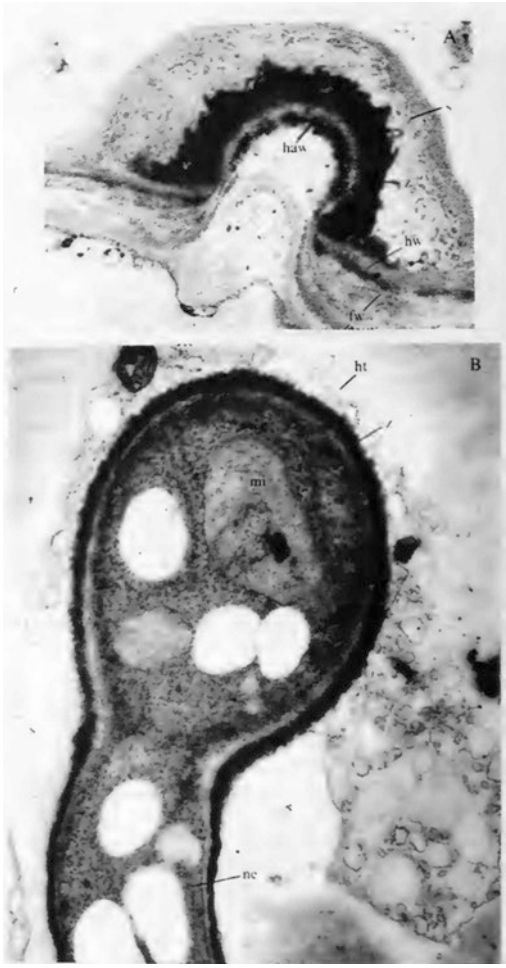

Plate 4.4 (**a**) Electron micrograph of a section of a haustorium initial in host mesophyll cell (section slightly oblique to the penetration zone), × 16500; (**b**) electron micrograph of a section of a very young haustorium in host epidermal cell showing breakdown of host cytoplasm into large number of vesicles, × 18000 (Chou 1970)

surface. The host plasmalemma covering the haustorium surface is often masked due to the accumulation of this substance (Plate 4.11a, d).

As soon as the haustorium penetrates the host, the haustorium becomes covered with a layer, moulded to its shape, and produced by the host protoplast (Fraymouth 1956). This layer is named 'The Sheath' and appears to be composed of modified cellulose and callose. A sudden increase in the growth rate of the fungus often causes the sheath to burst, remaining as a collar around the base. A morphologically analogous structure enveloping a haustorium initial which has penetrated the host wall (Plates 4.3c and 4.4a) has been detected in the cabbage – *Hyaloperonospora* system by Chou (1970). In mature haustoria which have differentiated into a neck and head, the sheath remains as a collar-like structure at the base (Plates 4.5 and 4.6) although completely ensheathed mature haustoria are sometimes observed under the light microscope (Plate 4.1d).

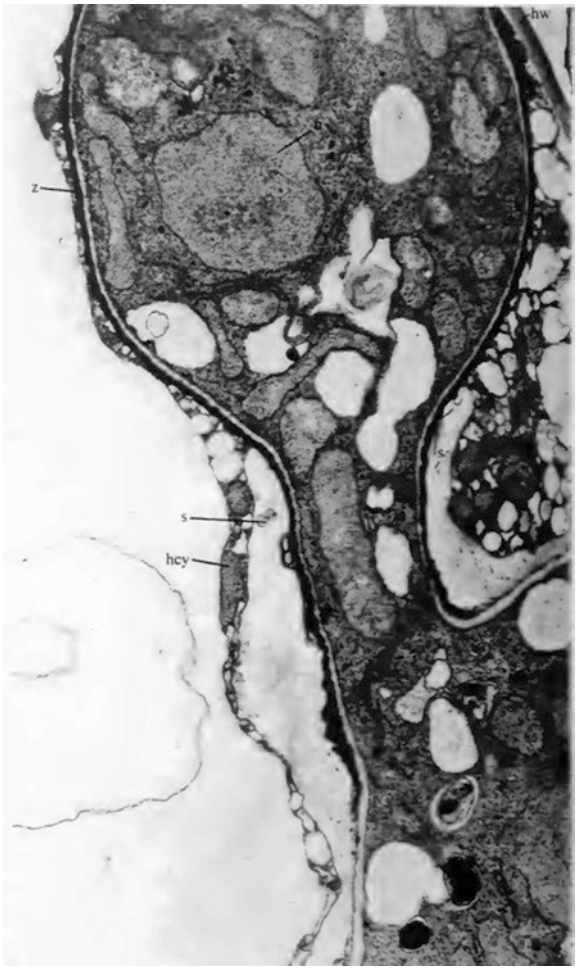

Plate 4.5 Electron micrograph of a section of a haustorium in host mesophyll cell at 6 h after inoculation, x 1 2000 (Chou 1970)

Electron microscope observation revealed that the sheath is a saclike structure sometimes flattened to a narrow strip (Plate 4.5), but in most cases dilated to a broadly conical shape and quite distinct in texture and electron density from the host wall. The sheath is bounded by a unit membrane which is generally presumed to be the host plasmalemma. No membranous structure can be detected along the sheath/host wall interface, though the two can be clearly distinguished by their difference in electron density and texture. The sheath matrix is electron transparent, while the host wall is moderately electron dense and often exhibits a fibrillar structure (Plate 4.2a). The sheath matrix is always permeated by large numbers of blurred electron-dense granules and dense vesicles with single or double membranes. These vesicles appear to be of host origin, as they are also found in the adjacent host cytoplasm (Plates 4.7b, d and 4.6). The sheath matrix is also interspersed with host cytoplasm (Plate 4.7d) which occurs in isolated packets or as an extension of the adjoining host

Plate 4.6 Electron micrograph of a section of a haustorium in host mesophyll cell at 6 h after inoculation, showing the saclike sheath and numerous vesicles (arrow pointed) and intra-vacuolar vesicles (pointed out by double arrow) in the sheath matrix, × 8580 (Chou 1970)

cytoplasm. The permeation of vesicles into the sheath matrix and the extension of host cytoplasm within it suggest a liquid or semi-liquid state of the sheath matrix (Fraymouth 1956; Chou 1970).

During penetration, the host cytoplasm adjoining the sheath increases markedly in amount and comes to contain a large number of vacuoles (Plates 4.5, 4.6 and 4.8a, c) (Chou 1970). At an early stage of haustorium development, coalescence of these vacuoles with the sheath can be seen. Intrusion of intra-vacuolar vesicles in the host cytoplasm and in the sheath can be seen (Plates 4.6 and 4.7a, c).

The ultrastructure of the interface between *H. arabidopsidis* and *A. thaliana* has very nicely been described by Mims et al. (2004). The diagrammatic representation

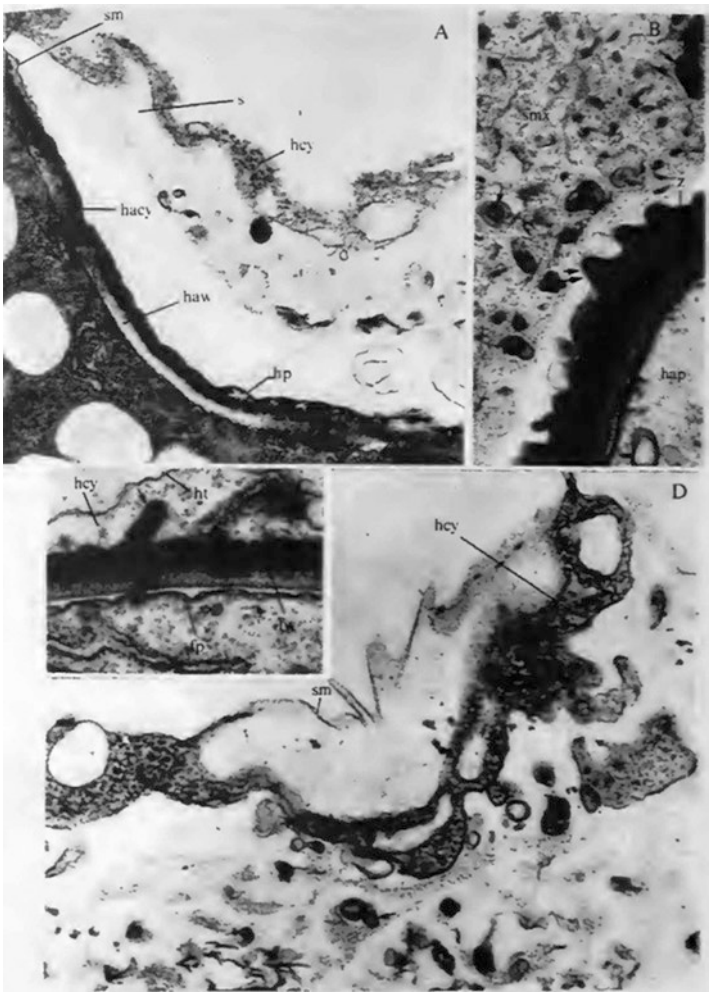

Plate 4.7 (**a**) Electron micrograph of a section of part of haustorium neck and sheath, × 24600; (**b**) electron micrograph of a section of part of haustorium neck and sheath showing numerous vesicles (arrow pointed) and dense granules in the sheath matrix (Smx) and the dentate extensions (pointed out by double arrow) of the dense zone (z) of haustorium wall, × 33000; (**c**) electron micrograph of a section of the interface between haustorium and host cytoplasm showing a dense vesicle (arrow pointed) like the secretary body, × 33000; (**d**) electron micrograph of a section of haustorium sheath showing incorporation of host cytoplasm (arrow pointed) in the sheath matrix and numerous membrane-bounded vesicles both in host cytoplasm and the sheath matrix, × 33000 (Chou 1970)

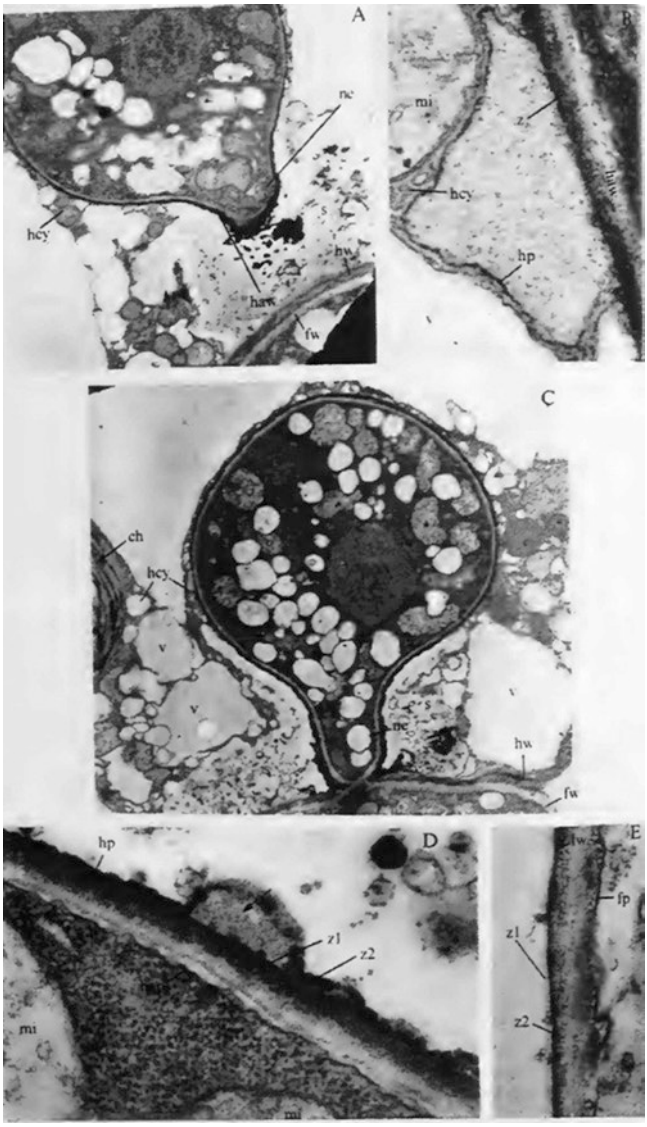

Plate 4.8 (**a**) Electron micrograph of a section of haustorium in host mesophyll cell showing the vacuoles or pro-vacuoles possibly in the process of fusion with each other and also with the sheath (arrow), × 7200; (**b**) electron micrograph of a section of the interface between haustorium and host cytoplasm showing vesiculation of the host plasmalemma, × 48000; (**c**) electron micrograph of a section of haustorium in host mesophyll cell showing fusion of vacuoles in host cytoplasm and sheath formation, × 7200; (**d**) electron micrograph of a section of interface between haustorium and host cytoplasm showing the structure of outer dense zone of haustorium wall distinguished into two well-defined layers (z1) and (z2), × 49500; (**e**) electron micrograph of a section of intercellular hyphae showing the hyphal wall also exhibiting a dense outer layer composed of z1 and z2 × 33000 (Chou 1970)

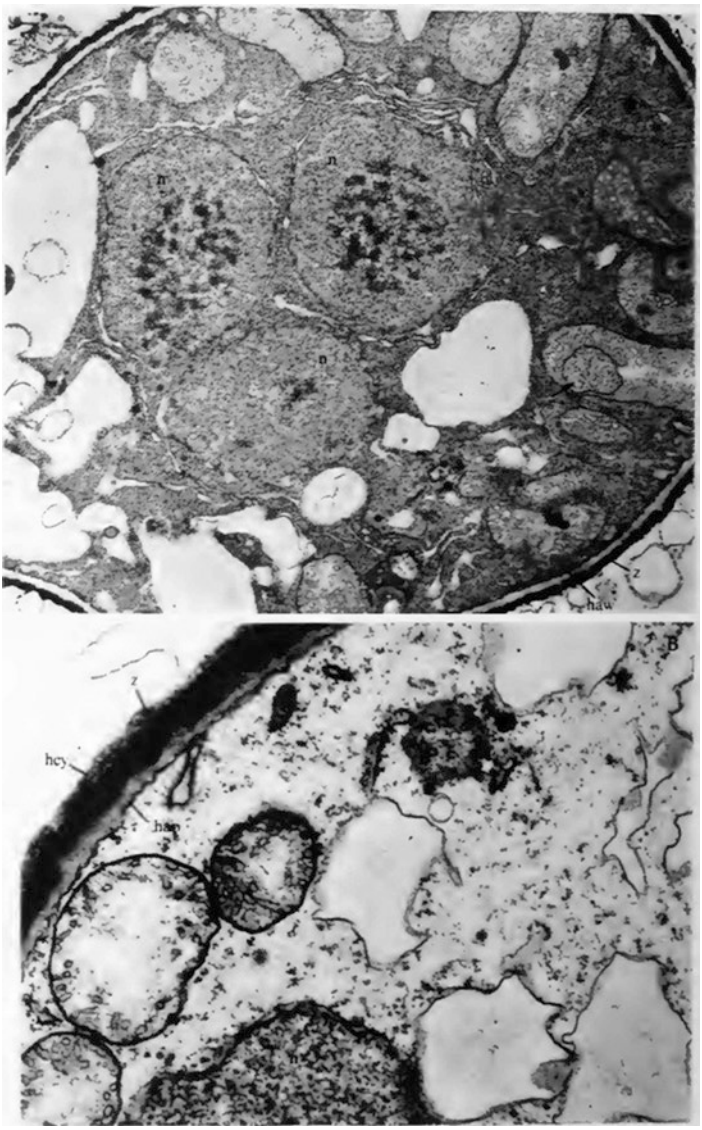

Plate 4.9 (**a**) Electron micrograph of a section of haustorium in epidermal cell at 6 h after inoculation showing the typical fine structure of haustorium at this stage. Ring formation in mitochondria pointed out by arrow, × 13200; (**b**) electron micrograph section of haustorium in epidermal cell 45 h after inoculation, × 24000 (Chou 1970)

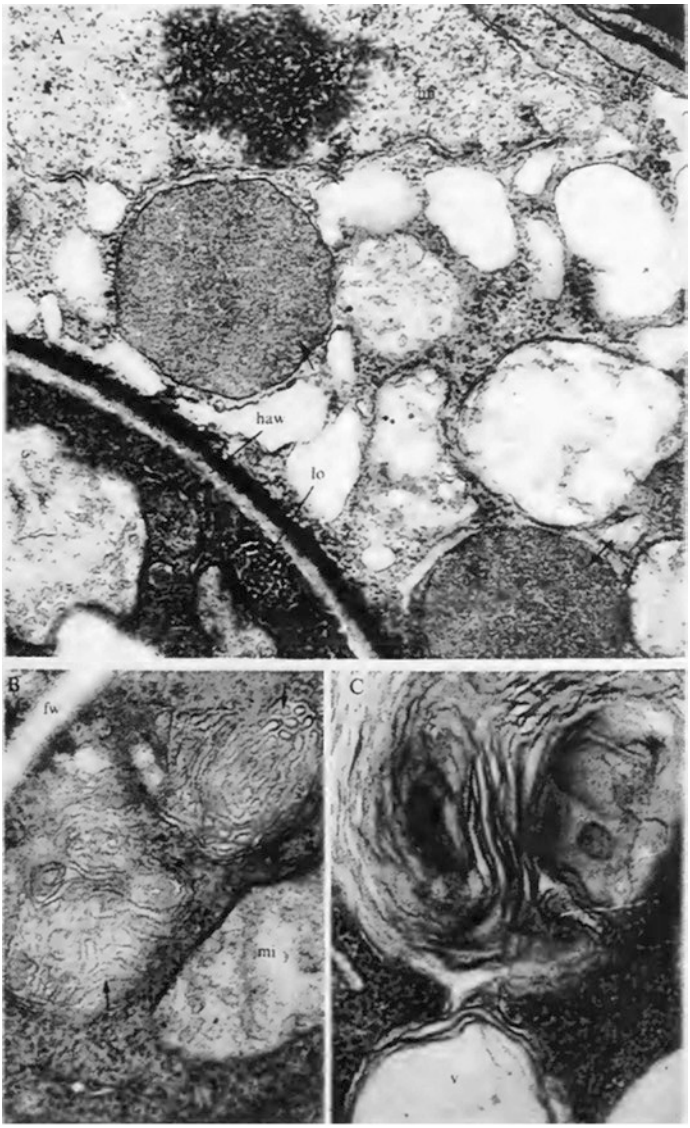

Plate 4.10 (**a**) Electron micrograph of a section of the interface between haustorium and host cytoplasm of mesophyll cell showing sphaerosome-like bodies (arrow pointed) in host cytoplasm, × 33000; (**b** and **c**) electron micrograph of sections of young penetrating hyphae, (**b**) showing complicated membrane system of unknown nature and (**c**) showing intra-vacuolar membrane systems, × 55200 and 36000, respectively (Chou 1970)

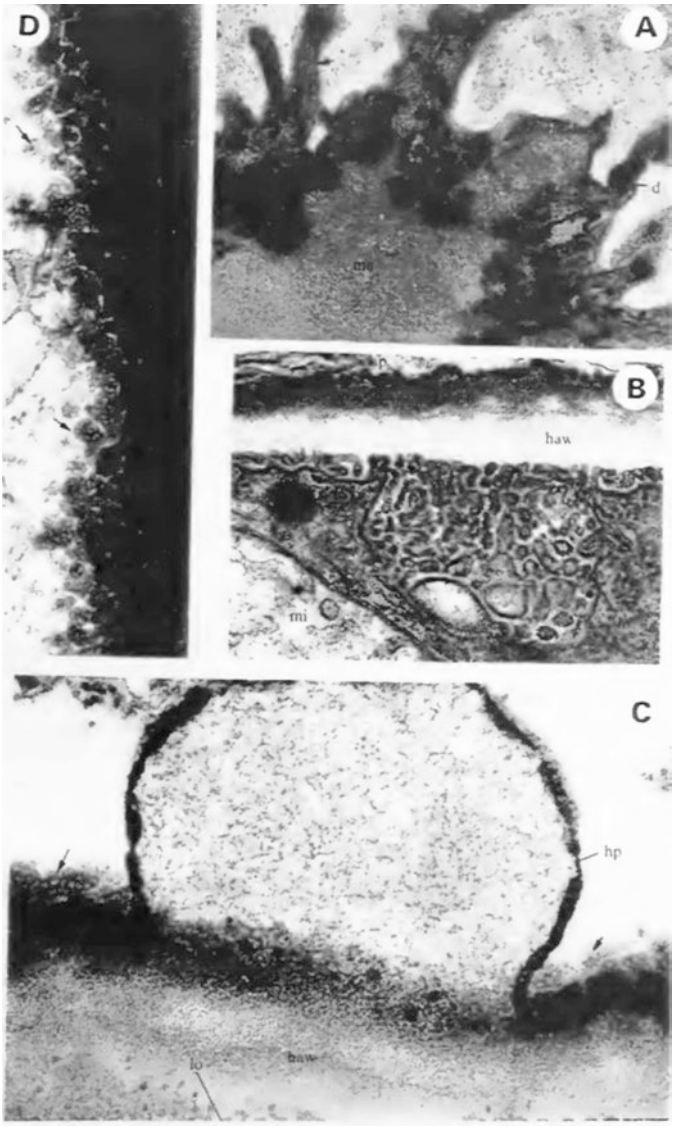

Plate 4.11 (**a**) Tangential section of the dense zone of haustorium neck showing foldings of host plasmalemma (arrow pointed) forming tubular extensions and incorporation of numerous dense granules (d), × 33000; (**b**) electron micrograph section of haustorium in host epidermal cell showing lomasome, × 55200; (**c**) electron micrograph of a section of haustorium in host epidermal cell showing pinocytotic vesicles formed from host plasmalemma and abundant porous substance (arrow pointed) at the host-parasite interface, × 73200; (**d**) electron micrograph section of interface between dense zone of haustorium and host cytoplasm showing the deposition of porous substance (arrow pointed), × 48000 (Chou 1970)

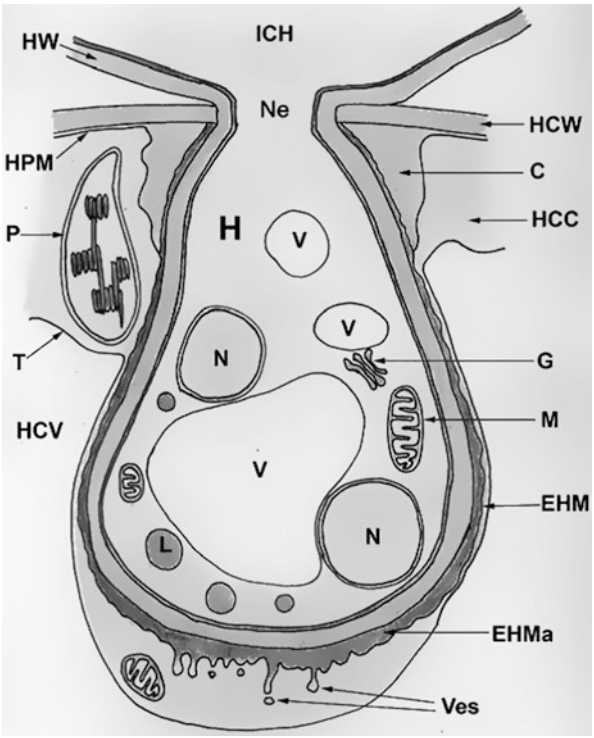

Plate 4.12 Schematic representation of a haustorium of *Hyaloperonospora arabidopsidis* in an *Arabidopsis* host cell (based on electron micrographs from Mims et al. 2004). C collar of host material (including callose), CC host cell cytoplasm, CV host cell vacuole, CW host cell wall, EHMa electron-dense extra-haustorial matrix, EHM extra-haustorial membrane, G Golgi body, H haustorium, HM hyphal membrane, HW hyphal wall, Ne neck region, PM host plasma membrane, HW hyphal wall, ICH intercellular hypha, L electron-dense lipid vesicle, M mitochondrion, N nucleus, Ne constricted neck region, P plastid, PM invaginated host cell plasma membrane, T tonoplast membrane of the host cell vacuole, V vacuoles in the haustorium, Ves vesicles either fusing with or budding off from the extra-haustorial matrix.

in Plate 4.12 revealed the vesicles (Ves) at the interface of the extra-haustorial matrix (EHMa) and the host cell cytoplasm (CC). It could be interpreted that these vesicles are budding off from, or coalescing with, the extra-haustorial membrane or both. Thus, these vesicles may represent a major mechanism and site of information/nutrient exchange between host and pathogen. The collar of host cell material could be decorated with immunogold particles labelled with a monoclonal antibody recognizing β-1,3-glucan epitopes showing that it is at least partially composed of callose. The host cell plasma membrane (PM) could be clearly observed to be invaginated by the haustorium, becoming the EHM. Other interesting features of the haustorium are the presence of multiple vacuoles and several nuclei. Golgi bodies, which are absent in true fungi but present in oomycete cells, were also clearly visible (Schlaich and Slusarenko 2009).

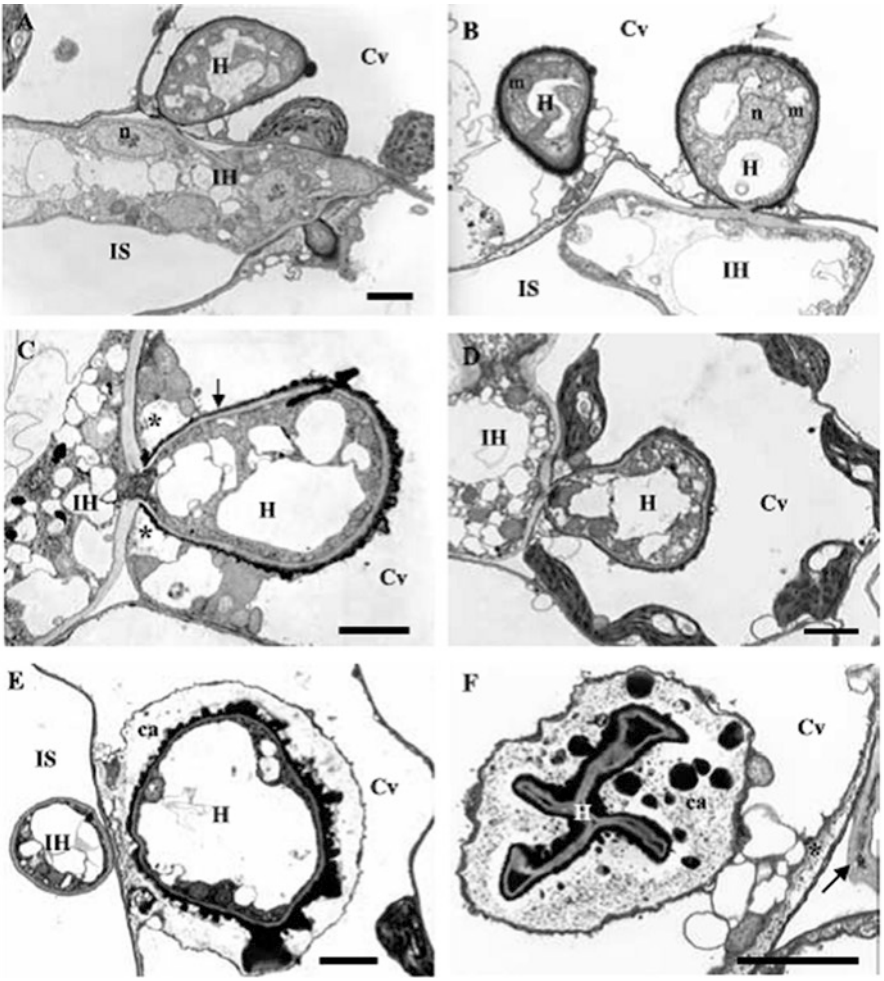

Plate 4.13 Ultrastructural features of the structures produced by *Hyaloperonospora parasitica* in susceptible accessions of *Arabidopsis*. Sections were taken from samples 3 (**a–d**), 5 (**e**), and 7 (**f**) days after inoculation. (**a**) Median section through a penetration site showing an intercellular hypha from which two haustoria penetrate two different host mesophyll cells of Ws-eds1. Note the presence of nucleus, lipid bodies, mitochondria, and large vacuoles in the intercellular hyphae. (**b**) Median section through a penetration point and two haustorial bodies in a host mesophyll cell of Ws-eds1. Note that the old haustorium (with haustorial neck) contains organelles such as mitochondria and nucleus. (**c**) Median section through a penetration point and haustorium in a mesophyll cell of Oy-0. Callose deposition (*) occurred at the penetration point around the proximal region of the haustorial neck. Note the presence of mitochondria and small and large vacuoles in the haustorium. The wall of the intercellular hypha is at its thickest where it penetrates the host cell wall to form the haustorial neck. The extra-haustorial matrix (arrows) is present around the haustorium. (**d**) Median section through a haustorium within the mesophyll cell of Ws-eds1. The cytoplasm of the intercellular hypha and haustorium contains mitochondria, lipid bodies, and small and large vacuoles. The host mesophyll cell appears unaffected by the presence of the haustorium as organelles are well preserved. (**e**) and (**f**) Callose deposition in Oy-0 (**e**) and Ws-eds1 (**f**). Callose

4.5 Ultrastructural Features of Intercellular Hyphae, Haustorium, and Host Cell

Observation of infected tissue under transmission electron microscopy (TEM) revealed the coenocytic hyphae, with an average diameter of 7.2 μm, ramified, and spread intercellularly throughout the host tissue (Plate 4.13a). The cytoplasm of intercellular hyphae was bounded by the pathogen plasma membrane and contained many ribosomes, endoplasmic reticulum (ER), lipid bodies, mitochondria, and nuclei. Small and large vacuoles containing moderately electron-dense material occupied a significant volume of the hyphae (Plate 4.13a–d). Further growth of hyphae within intercellular spaces and penetration of individual host mesophyll cells have been resulted in the formation of haustoria.

Intracellular haustoria were large and lobate with an average diameter of 5.4–7.1 μm. A typical mature haustorium is differentiated into a very short neck and head (Plate 4.13c, d). The haustorial neck is constricted at the penetration site, ranging in width from approximately 0.4 to 0.95 lm. Callose-like deposits were frequently observed at sites of penetration around the proximal region of the haustorial neck (Plate 4.13c). Median sections through penetration sites revealed that the pathogen wall was continuous from the intercellular hypha along the entire haustorial body (Plate 4.13c, d). The cell wall consisted of a single layer that was thicker around the intercellular hyphae (0.34 μm) compared with that around the haustorial body (0.18 μm). The pathogen plasma membrane was continuous from the intercellular hypha throughout the haustorium and was tightly pressed to the haustorial wall. Haustoria in infected cells were surrounded by an invagination of the host plasma membrane, the extra-haustorial membrane (EHM). EHM is separated from the pathogen wall around the haustorial body by an electron-dense extra-haustorial matrix (Plate 4.13c). The extra-haustorial matrix is a non-cytoplasmic part of haustorium. This region was variable in width up to approximately 0.3 μm thick and was located around the haustoria and the neck region (Plate 4.13c). The cytoplasm of the haustorium contained organelles, which were similar to that of the intercellular hyphae. Large vacuoles were common in hyphae and older haustoria (Plate 4.13a–e). The haustorial body contained more mitochondria than other parts of pathogen (Plate 4.13a). One nucleus with dense heterochromatic regions was observed in haustoria but is not a constant feature (Plate 4.13b).

During the early stages of infection, one to two haustoria were often observed in single mesophyll cells (Plate 4.13a, b), but as many as four to five haustorial profiles were found within a single cell at 5 dai. Organelles within the penetrated host cell

Plate 4.13 (continued) deposition stained lightly around the haustorium shown in (**e**) but densely around the haustorium and in the cell wall (*) shown in (**f**). Note that contents of the haustorium and infection hypha appear normal during the early stage of infection (**e**) as organelles are clearly distinguished in the host cytoplasm. The contents of the haustorium and the infection hypha (arrow) became necrotic at the late stage of infection (**f**). All bars ¼ 3 lm. *H* haustorium; *IH* intercellular hypha; *IS* intercellular space; *m* mitochondrion; *n* nucleus; *ca* callose; *Cv* cell vacuole (Soylu and Soylu 2003)

did not appear to be affected following formation of haustoria (Plate 4.13d). The region around and between the haustoria contained an abundance of cytoplasm with many vesicles, plastids, mitochondria, and microbodies. Occasionally, ensheathed healthy haustoria were observed at infection sites. In general, the cytoplasm of the ensheathed haustorium and associated intercellular hypha were apparently normal at 5 dai (Plate 4.13e). By 7 dai, however, ensheathed haustoria and associated intercellular hypha became necrotic as evident by their misshapen, irregular appearance, and dense contents (Plate 4.13f) (Soylu and Soylu 2003).

Certain ultrastructural features of the haustorial apparatus of *H. parasitica* on susceptible *Arabidopsis* plants do not resemble those of *H. parasitica* on cabbage (Chou 1970) and other relevant *Peronospora* species such as *Peronospora pisi* in pea plants (Hickey and Coffey 1977). Ultrastructural features of the *H. parasitica* haustorium clearly distinguish the pathogen from the downy mildews in other crops. Unlike other downy mildews, which produce simple, cylindrical haustoria with a narrow cylindrical long neck, the complete structural unit of a haustorium produced by *H. parasitica* consists of a lobe-shaped haustorial head and extra-haustorial matrix in the absence of an apparent haustorial neck. Features of coenocytic intercellular hyphae were similar to those of other downy mildew pathogens. The cytoplasm of intercellular hyphae contained typical organelles characteristic of the pathogen. Large vacuoles containing moderately electron-dense material occupied a significant volume of the hyphae. The pathogen cell wall consisted of single layer of consistent thickness around the intercellular hyphae except at the penetration points where it was frequently thicker. As described for other downy mildews (Chou 1970; Hickey and Coffey 1977), the haustorial body contained a normal complement of organelles, usually including one to two nuclei.

Observation of several median sections of haustoria revealed that the hyphal wall appears to be continuous from the intercellular hypha at the penetration sites, then through the host wall, and finally around the haustorial body. Median sections through penetration sites revealed the presence of cell wall depositions (papillae) at the site of penetration. Aniline blue fluorescence confirmed the presence of callose-like material in these depositions. Callose-like deposits or papillae are frequently reported at sites of penetration by other species of Peronosporales (Hickey and Coffey 1977; Sargent 1981; Woods et al. 1988; Cohen et al. 1989; Enkerli et al. 1997). Deposition of papillae adjacent to the penetrating haustoria represents a non-specific host cytoplasmic response to both mechanical and pathogenic injury (Ingram et al. 1976).

Among obligate fungal pathogens, the invagination of the plasma membrane by a haustorium has been termed the EHM. In *H. parasitica*, the haustorium was also surrounded by an EHM. The EHM has been shown to differ from the host plasma membrane in a number of aspects (Spencer-Phillips and Gay 1981; Roberts et al. 1993). However, at penetration sites, a clear continuity between the membrane binding the dense staining matrix and the plasma membrane was not always definitely established. The EHM is separated from the fungal structures in the haustorium by a gel-like substance termed the extra-haustorial matrix. The extra-haustorial matrix completely surrounded the haustorium of *H. parasitica* (Soylu and Soylu 2003).

4.6 Conidiophore Development

Conidiophore development of *H. parasitica* can be divided into five stages (Davison, Davison 1968a, b, c).

4.6.1 Conidiophore Primordial

The emergence of *H. parasitica* from the host cotyledons during sporulation can be seen as a densely stained region beneath the host stomata. In the sub-stomatal space, a hyphal branch, about 5 μm in diameter, grows towards the stoma and then between the guard cells (Plate 4.14a). When the tip of this hypha is about level with the top of the guard cells, it becomes more rounded and completely blocks the stomatal pore (Plate 4.14b). It is referred to as conidiophore primordium. According to Shiraishi et al. (1975), a contracted image is found in the region when the conidiophores develop.

4.6.2 Unbranched Conidiophores

It is the earliest stage of conidiophore development visible on the surface of the host and can be seen about 4 h after the cotyledons are placed in a moist, dark environment. From the primordia, unbranched conidiophores may develop immediately, or a narrow wall surrounding a 'blowout' forms at the apex (Plate 4.14b). The basal constriction surmounted by a bulge which is observed in older conidiophores is probably the result of the 'blowout' formation. Developing conidiophores are more or less cylindrical at this stage (Plate 4.14c), approximately 10–12 μm in diameter and of varying length.

4.6.3 Production of Branches

When the conidiophores reach about two third of its eventual height, branches are formed one at a time, just behind the conidiophore apex (Plate 4.14d). Secondary and tertiary branches are also formed which are narrower than the primary ones. The conidiophore axis is also narrower at the apex, with decrease in branch diameter being proportional to the increase in branch length. The ultimate branches are very slender, often about 1 μm in diameter, and usually curved. Branches form at a projected angle of 55–85° with the major axis, and the number produced is approximately proportional to the conidiophore height.

4.6.4 Development of Conidia

Young conidia are formed about 2 h after initiation of branch production. Initially, conidia are spherical, but as they increase in size, they become ellipsoidal (Plate 4.14e). Conidia produced on a single conidiophore are of uniform size, but conidia borne by different conidiophores frequently vary in size.

4.6.5 Formation of a Cross Wall

Conidia are delimited by a cross wall about 2 h after the beginning of conidial formation, when they reach about 15 × 20 µm in size (Plate 4.14h). However, the cross walls are observed only occasionally since spores are usually detached before cross wall formation.

4.6.6 Conidiophore Growth

The increase in conidiophore length shows an initial slow period of elongation, just after the fungus has emerged from the host leaf followed by a rapid increase (Plate 4.15; Figs. 4.1 and 4.2). During branch formation, increase in length is slightly slower and less regular, while just before spore formation, conidiophore elongation slows down and almost ceases. Once formed, the spores enlarge rapidly, but increase in conidiophore length is only by the enlargement of the apical spore. The most rapid rate of elongation of conidiophores is 100–200 µm/h. As the branches usually begin about two third of the way up the final length of the conidiophore stalk, late conidiophores are usually shorter, are less profusely branched, and bear fewer spores than the conidiophores formed earlier. Although increase in volume may be approximately linear during the growth of unbranched conidiophores, and branch production, there is a decrease in the rate of volume increase just before spore formation. This is followed by a massive increase in volume just after spore formation, when the total conidiophore volume may be more than quadrupled (Fig. 4.3) depending on the number of spores produced. The inflation of the branch apex is a gradual process which occurs without any interruption (Fig. 4.4) in branch elongation (Davison 1968b).

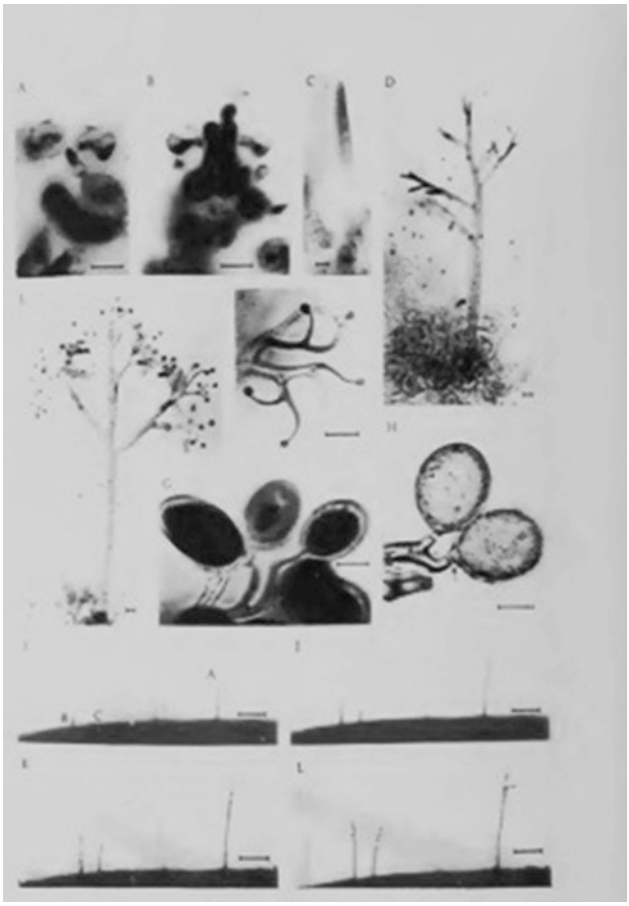

Plate 4.14 (**a**) Section of wax-embedded material showing a hyphal branch growing towards a stoma; (**b**) section of wax-embedded material illustrating two conidiophore primordia, one of which is beginning to grow; (**c**) stained and macerated preparation of an unbranched conidiophore; (**d**) stained and macerated preparation of a branched conidiophore; (**e**) a branched conidiophore with small spores in a stained and macerated preparation; (**f**) very young spores; (**g**) mature spores; (**h**) mature spores delimited by a cross wall (arrow); (1-L) frames from the cine film illustrating the development of conidiophores A, B, and C; (**i**) incubation time 3 h 30 min.; (**j**) incubation time 3 h 50 min.; (**k**) incubation time 4 h 10 min.; and (**l**) incubation time 4 h 30 min. A–H scale line is 10 μm; I–L scale line is 100 μm (Davison 1968b)

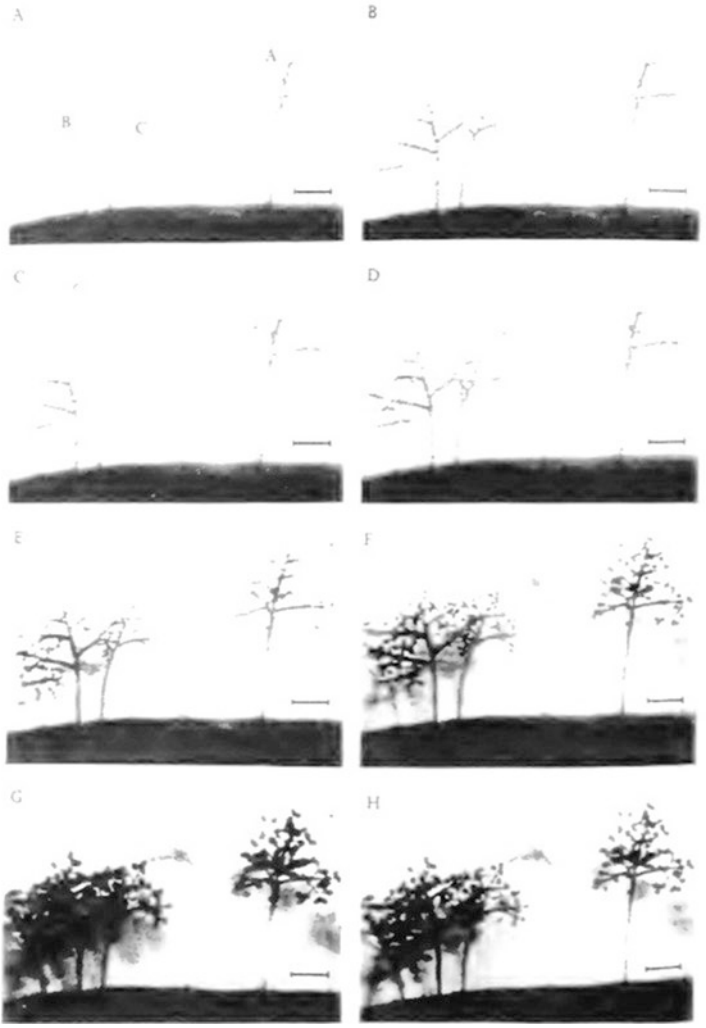

Plate 4.15 Continued development of conidiophores: (**a**) incubation time 4 h 50 min.; (**b**) incubation time 5 h 10 min.; (**c**) incubation time 5 h 30 min.; (**d**) incubation time 5 h 50 min.; (**e**) incubation time 6 h 10 min.; (**f**) incubation time 6 h 30 min.; (**g**) incubation time 6 h 50 min.; and (**h**) incubation time 7 h 30 min. Scale line is 100 μm (Davison 1968b)

4.6.7 Conidial Formation

Surface ultrastructure of conidia, germ tubes, appressoria, and conidiophores of *H. parasitica* infecting Japanese radish has been observed by Shiraishi et al. (1974) through scanning electron microscopy (Plates 4.16, 4.17, 4.18 and 4.19). Mature conidia are approximately 7 μm in width and 10 μm in length. Conidia are formed directly from the swelling tips of the conidiophores, and they have the same surface structure as the conidiophores. Old conidia have many wartlike structures, although the mature conidiophores have a smooth surface (Plates 4.17 and 4.19).

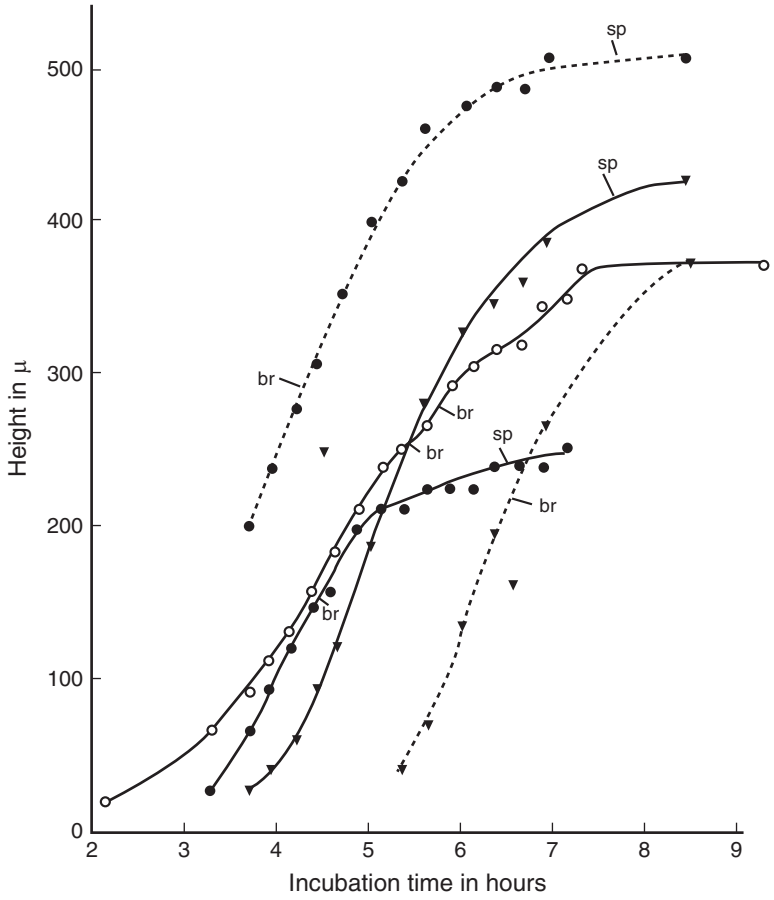

Fig. 4.1 Increase in length of five individual conidiophores growing in the humidity chamber; br, time at which branching commenced; sp., spore formation (Davison 1968c)

4.6.8 Host Response

The host protoplast of epidermal and mesophyll cells responds differently to infection by the downy mildew pathogen (Chou 1970). The epidermal cells in most cases respond vigorously to infection resulting in a severe disruption of the protoplast. The central vacuoles contract and undergo fragmentation. The plasmalemma is broken down or detached from the wall, and numerous vesicles are formed from it. The cytoplasm, which originally appeared as a thin peripheral coating of the wall, is either dislocated and aggregated into a vacuolated blob or completely dispersed to the extent that its identity cannot be discerned. Apparently intact mitochondria and chloroplasts appear to be set free from the groundplasm. Consequently, haustoria in epidermal cells are not surrounded by a clearly defined layer of host cytoplasm. Haustoria formation in a mesophyll cell is less disruptive. The host cytoplasm is invaginated by the invading haustorium, while the tonoplast and plasmalemma remain intact.

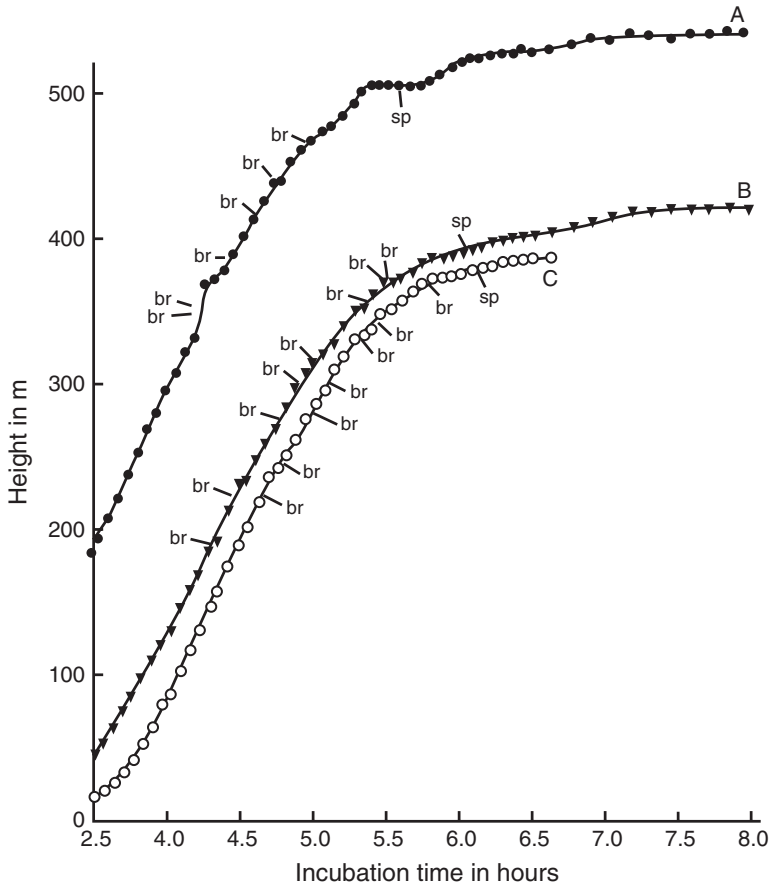

Fig. 4.2 Increase in length of conidiophores *A*, *B*, and *C*. br, formation of primary branch; sp., spore formation (Davison 1968c)

4.6.9 Cytology and Genetics

The haploid chromosome number of *H. parasitica* is n = 18–20 and it is a tetraploid (Sansome and Sansome 1974). Nuclei, mitochondria, lipid material, protein, and RNA in the intercellular mycelia and haustoria of *H. parasitica* are uniformly distributed (Davison 1968a). Insoluble carbohydrate material has been detected in the fungal cell wall. Callose sheaths are occasionally seen partially surrounding the haustoria. A distinct plasmalemma, porate nuclei, tubular endoplasmic reticulum,

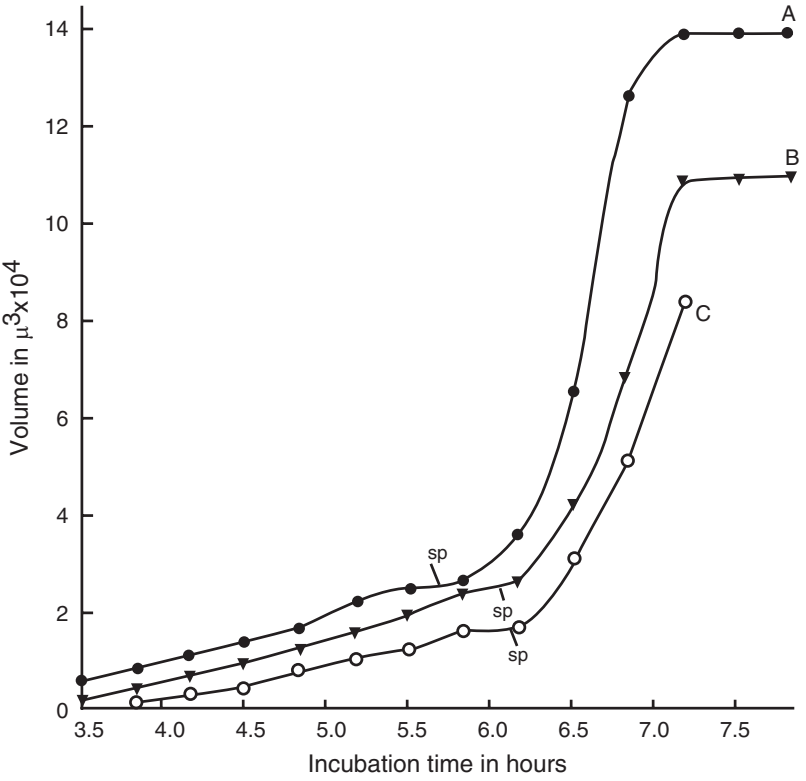

Fig. 4.3 Increase in volume of conidiophores A, B, and C. sp., spore formation (Davison 1968c)

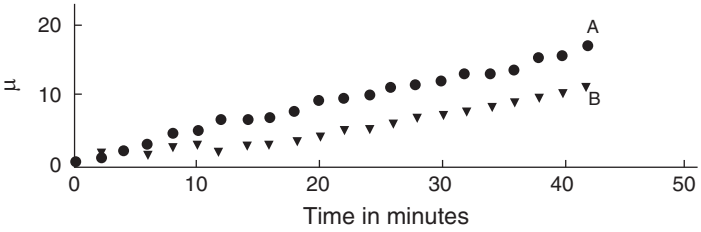

Fig. 4.4 Increase in branch length and apical diameter during spore formation. *I* branch length, *b* apical diameter (Davison 1968c)

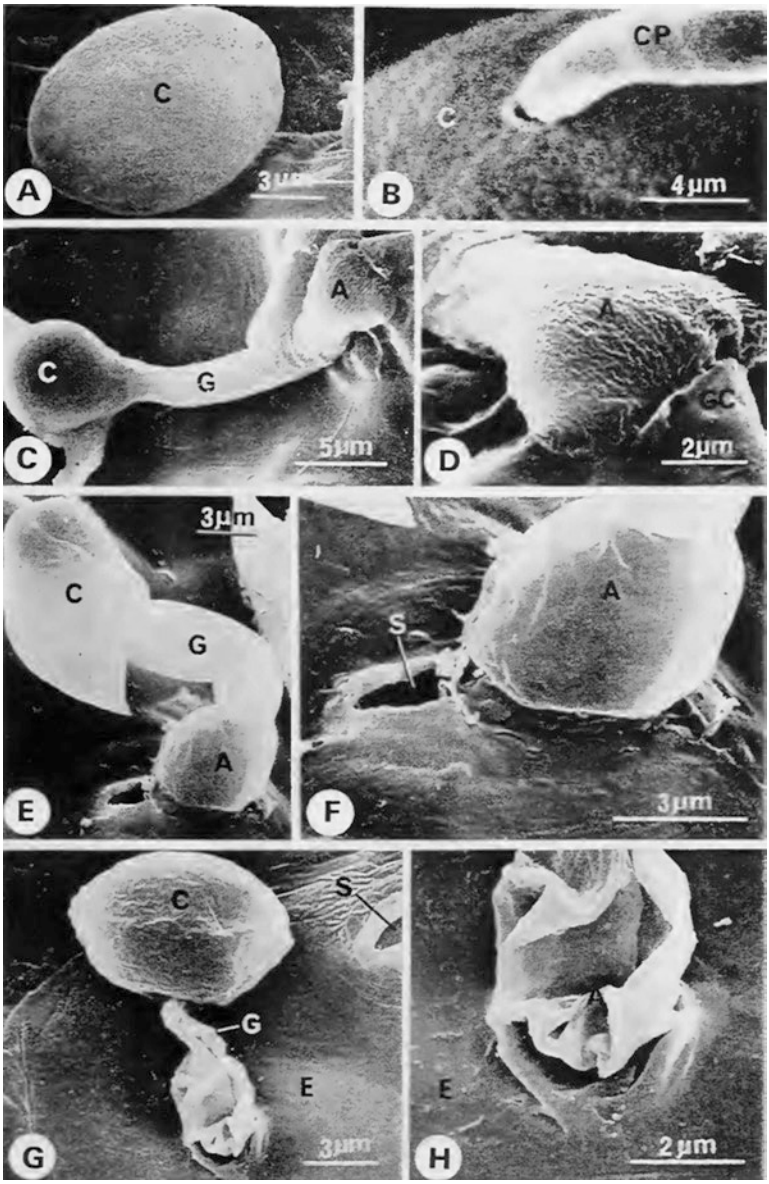

Plate 4.16 Electron micrograph of conidia, germ tubes, and initial period of *Hyaloperonospora parasitica* invasion on Japanese radish leaves. (**a**) Mature conidium. The surface is rough, with wart-shaped structure; (**b**) separation of a mature conidium from its conidiophore; (**c**) an appressorium above a stoma and a penetration peg into the stomatal cavity; (**d**) enlargement of C. Wrinkly structures on an appressorium in the initial period of formation; (**e**) an appressorium over a stoma 48 h after germination; (**f**) enlargement of E. Slight degeneration of the epidermal cells where the appressorium is in contact with the stomatal guard cells; (**g**) cuticular invasion. Germ tube growing from the side of a spore; (**h**) enlargement of G. The appressorium is quite contracted (Shiraishi et al. 1975)

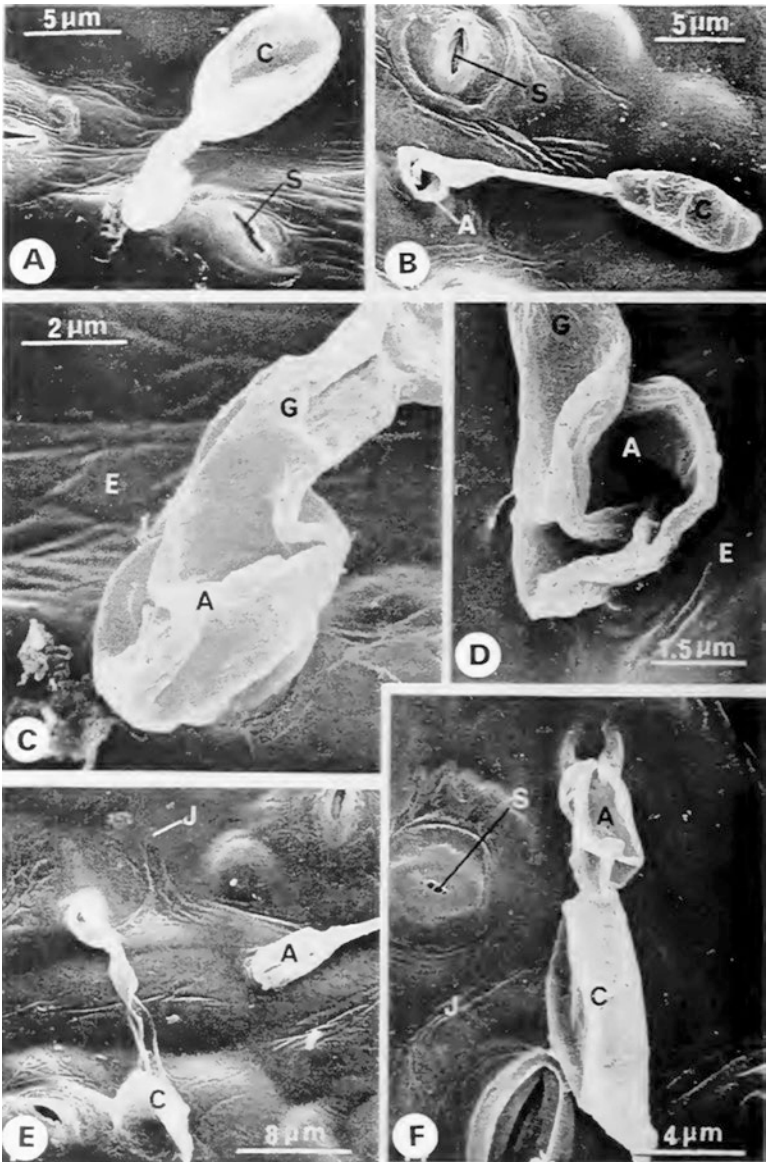

Plate 4.17 Electron micrograph of initial period of *Hyaloperonospora parasitica* invasion on Japanese radish leaves. (**a**) Invasion through a junction between a stomatal guard cell and an auxiliary cell; (**b**) cuticular invasion of an auxiliary cell. The germ tube is quite extended, but invasion does not depend on a stoma being present; (**c**) enlargement of B. The viscous substance used by the appressorium to adhere to the epidermal cell wall is not very visible; (**d**) enlargement of C. The germ tube and appressorium are clearly contracted, and circular traces of where the penetration peg has entered can be seen in the epidermal cell wall; (**e**) cuticular invasion with a long germ tube; (**f**) cuticular invasion through a short germ tube. Although the conidium is adjacent to a stoma, germination has occurred from the conidium wall on the side away from the stoma, and cuticular invasion is taking place (Shiraishi et al. 1975)

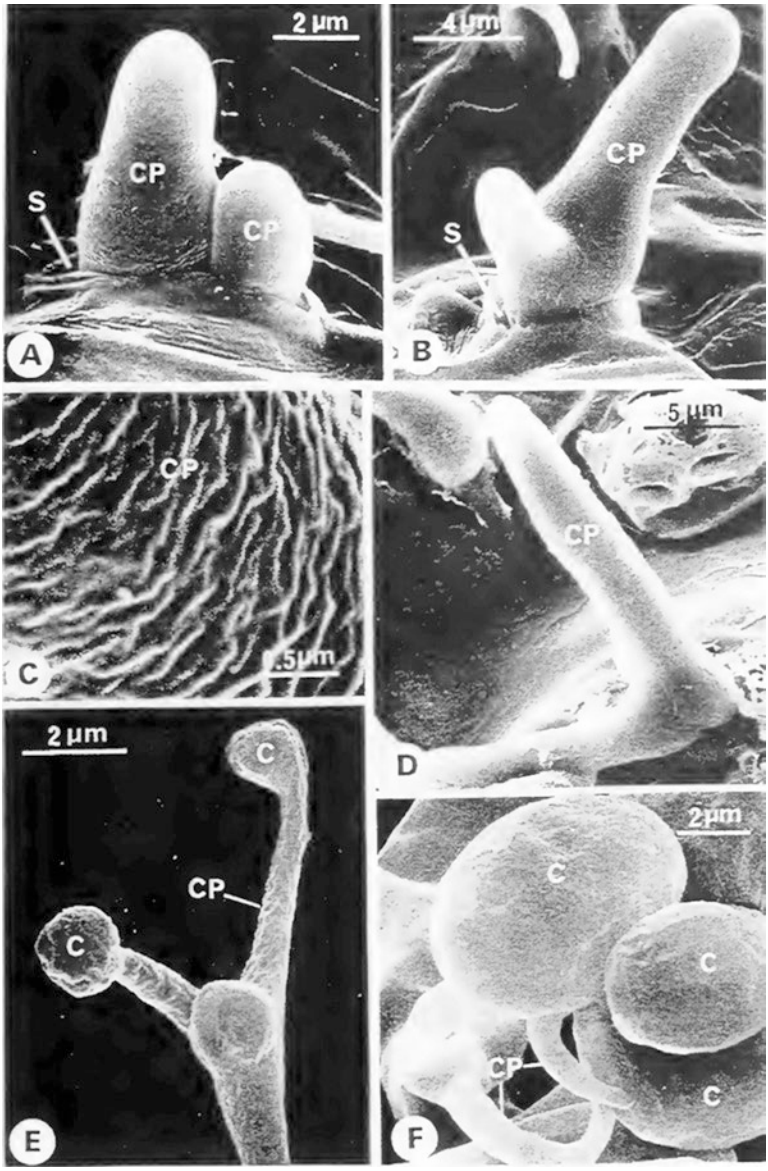

Plate 4.18 Electron micrograph showing development of conidiophores and conidia of *Hyaloperonospora parasitica* on Japanese radish leaves. (**a**) Conidiophores invariably grow out of stomata, sometimes two at a time; (**b**) a conidiophore branching during the initial stage of new growth; (**c**) surface of a conidiophore during the initial stage of new growth, with a wavy structure; (**d**) an extended conidiophore with appearance of a crimp at the base; (**e**) initial stage of conidium formation. The tips of the conidiophore swell, forming conidia. The conidiophores and conidia have similar surface structures; (**f**) clusters of conidia that have matured and begun to take on a tuft-like shape (Shiraishi et al. 1975)

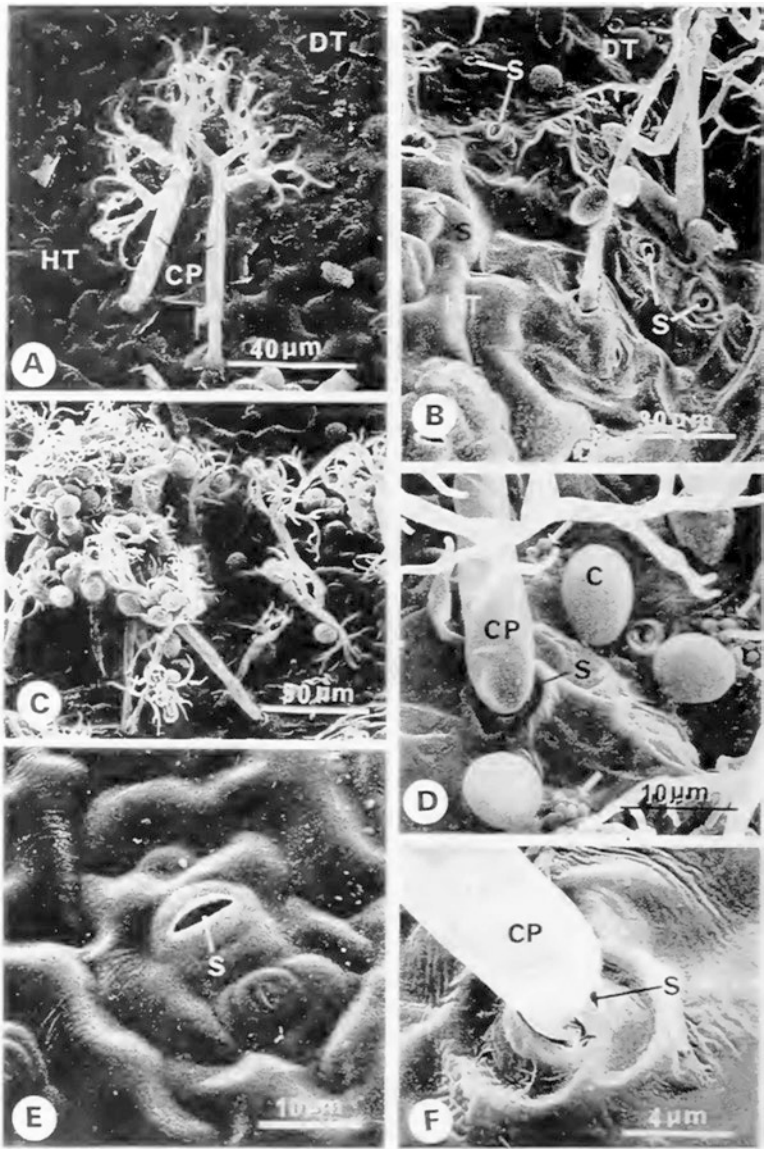

Plate 4.19 Electron micrographs showing conidiophores and conidia of *Hyaloperonospora parasitica* on Japanese radish leaves. (**a**) Conidiophores without conidia. The area at the top right is a relatively young diseased area, and exfoliation of epidermal cell wax and cuticular material can be seen; (**b**) diseased area with advanced signs of disease. Wrinkles have appeared in the epidermis of the diseased area, and open stomata can be seen; (**c**) diseased area with many developed conidiophores; (**d**) diseased area with advanced symptoms of disease. A crimp in the base of the conidiophore is visible. Yeast-shaped fungi are also present; (**e**) stoma in a healthy area. It is formed of two stomatal guard cells and several auxiliary cells; (**f**) the base of the conidiophore is crimped, perhaps due to mechanical force exerted by the stoma. Wrinkles on the surface of the host are clearly visible (Shiraishi et al. 1975)

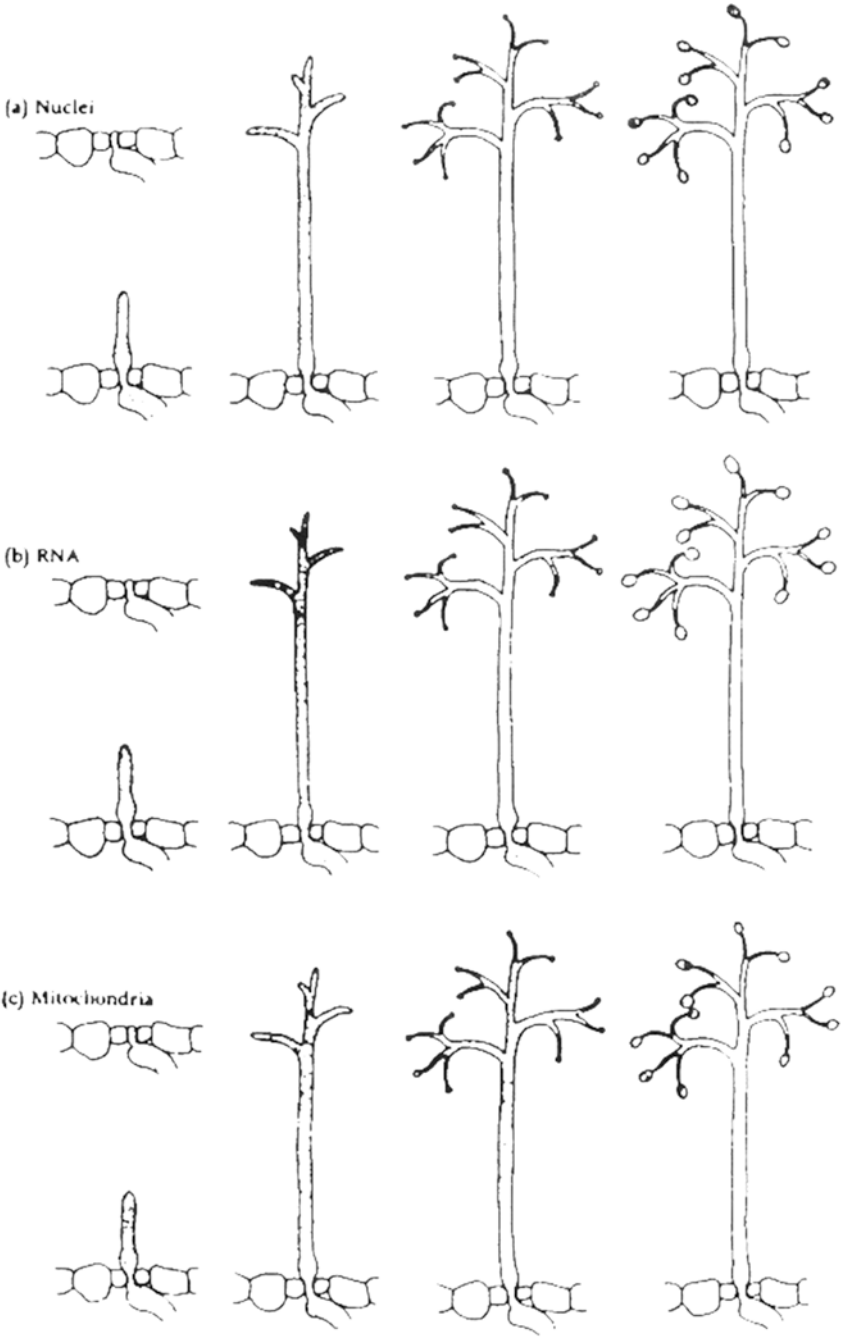

Fig. 4.5 The distribution of (**a**) nuclei, (**b**) RNA, and (**c**) mitochondria in the developing conidiophores of *Hyaloperonospora parasitica* (Davison 1968c)

mitochondria with tubular cristae, Golgi dictyosomes, and lipid bodies are present within the protoplast (Ehrlich and Ehrlich 1966). The distribution of organelles, storage products, and other substances within the developing conidiophores of *H. parasitica* is very different from the distribution observed within the intercellular mycelium (Davison 1968c). In developing conidiophores, the nuclei, mitochondria, protein, and lipid material are more or less uniformly distributed at first, but gradually shift into the conidia so that by maturity all these substances have relocated, leaving the conidiophore stalk and branches almost completely empty (Plate 4.19; Figs. 4.5, 4.6 and 4.7). Glycogen has not been detected within conidiophores or conidia of *H. parasitica*. Trehalose and either glucose or mannose are identified in the conidiophores and conidia of *H. parasitica* but sugar alcohols are absent.

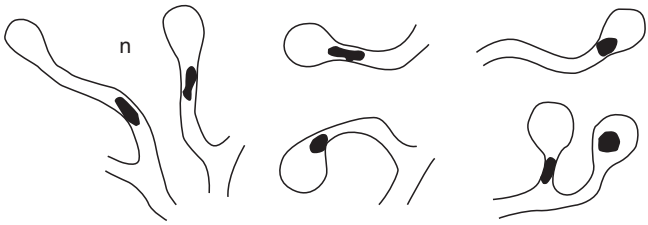

Fig. 4.6 Migration of nuclei (n) into the nucleate spores of *Hyaloperonospora parasitica* (Davison 1968c)

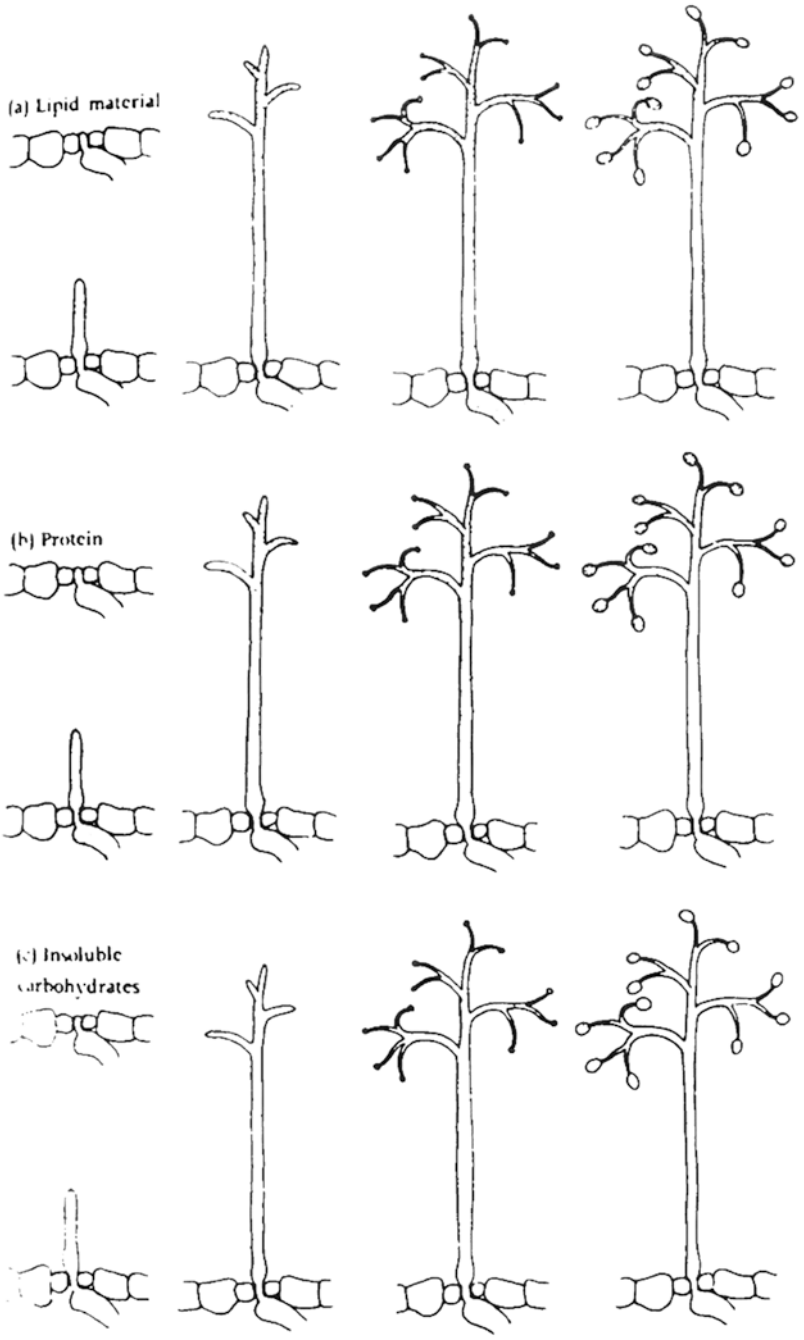

Fig. 4.7 The distribution of (**a**) lipid material, (**b**) protein, and (**c**) insoluble carbohydrates in the developing conidiophores of *Hyaloperonospora parasitica* (Davison 1968c)

References

Chou CK (1970) An electron-microscope study of host penetration and early stages of haustorium formation of *Peronospora parasitica* (Fr.) Tul. on cabbage cotyledons. Ann Bot 34:189–204

Cohen Y, Eyal H, Hanania J, Malik Z (1989) Ultrastructure of *Pseudoperonospora cubensis* in muskmelon genotype susceptible and resistant to downy mildew. Physiol Mol Plant Pathol 34:27–40

Davison EM (1968a) Cytochemistry and ultrastructure of hyphae and haustoria of *Peronospora parasitica* (Pers. ex Fr.) Fr. Ann Bot 32:613–621

Davison EM (1968b) Development of sporangiophores of *Peronospora parasitica* (Pers. ex Fr.) Fr. Ann Bot 32:623–631

Davison EM (1968c) The distribution of substances in sporangiophores of *Peronospora parasitica* (Pers. ex Fr.) Fr. Ann Bot 32:633–647

Ehrlich MA, Ehrlich HG (1966) Ultrastructure of the hyphae and haustoria of *Phytophthora infestans* and hyphae of *Peronospora parasitica*. Can J Bot 44:1495–1504

Enkerli K, Hahn MG, Mims CW (1997) Ultrastructure of compatible and incompatible interactions of soybean roots infected with the plant pathogenic oomycete *Phytophthora sojae*. Can J Bot 75:1493–1508

Fraymouth J (1956) Haustoria of the Peronosporales. Trans Br Mycol Soc 39:79–107

Hickey EL, Coffey MD (1977) A fine-structural study of the pea downy mildew fungus *Peronospora pisi* in its host *Pisum sativum*. Can J Bot 55:2845–2858

Ingram DS, Sargent JA, Tommerup IC (1976) Structural aspects of infection by biotrophic fungi. In: Friend J, Threlfall DR (eds) Biochemical aspects of pant- and parasite relationships. Academic, London, pp 43–78

Mims CW, Richardson EA, Holt BF III, Jl D (2004) Ultrastructure of the host-pathogen interface in *Arabidopsis thaliana* leaves infected by the downy mildew *Hyaloperonospora parasitica*. Can J Bot 82:1001–1008

Roberts AM, Mackie AJ, Hathaway V, Callow JA, Green JR (1993) Molecular differentiation in the extrahaustorial membrane of pea powdery mildew haustoria at early and late stages of development. Physiol Mol Plant Pathol 43:147–160

Sansome E, Sansome FW (1974) Cytology and life history of *Peronospora parasitica* on *Capsella bursa-pastoris* and of *Albugo candida* on *C. bursa-pastoris* and on *Lunaria annua*. Trans Br Mycol Soc 62:323–332

Sargent JA (1981) The fine structure of the downy mildews. In: Spencer DM (ed) The downy mildews. Academic, London, pp 183–236

Schlaich NL, Slusarenko A (2009) Downy mildew of *Arabidopsis* caused by *Hyaloperonospora arabidopsidis* (formerly *Hyaloperonospora parasitica*) (Chapter 13). In: Kurt L, Kamoun S (eds) Oomycete genetics and genomics: diversity, interactions and research tools. Wiley, Hoboken, pp 263–285

Shiraishi MK, Sakamoto S, Asada Y (1974) An electron microscope study of Japanese radish leaves infected with *Peronospora parasitica*. Mem Coll Agric Ehime Univ 19:137–168

Shiraishi M, Sakamoto K, Asada Y, Nagatani T, Hidaka H (1975) A scanning electron microscopic observation on the surface of Japanese radish leaves infected by *Peronospora parasitica* (Fr.) Fr. Ann Phytopathol Soc Japan 41:24–32

Soylu EM, Soylu S (2003) Light and electron microscopy of the compatible interaction between *Arabidopsis* and the downy mildew pathogen *Peronospora parasitica*. J Phytopathol 151:300–306

Spencer-Phillips PTN, Gay JL (1981) Domains of ATPase in plasma membranes and transport through infected plant cells. New Phytol 89:393–400

Woods AM, Didehvar F, Gay JL, Mansfield JW (1988) Modification of the host plasmalemma in haustorial infections of *Lactuca sativa* by *Bremia lactucae*. Physiol Mol Plant Pathol 33:299–310